Sciencexpress Research Article

Bypassing a Kinase Activity with an ATP-Competitive Drug

Feroz R. Papa,[1,3]* Chao Zhang,[2] Kevan Shokat,[2] Peter Walter[3]

Howard Hughes Medical Institute[3], and Departments of Medicine[1], Cellular and Molecular Pharmacology[2], Biochemistry and Biophysics[3]. University of California, San Francisco, San Francisco, CA 94143–2200, USA.

*To whom correspondence should be addressed. E-mail: frpapa@medicine.ucsf.edu

Unfolded proteins in the endoplasmic reticulum cause *trans*-autophosphorylation of the bifunctional transmembrane kinase Ire1, which induces its endoribonuclease activity. The endoribonuclease initiates non-conventional splicing of *HAC1* mRNA to trigger the unfolded protein response (UPR). We explored the role of Ire1's kinase domain by sensitizing it through site-directed mutagenesis to the ATP-competitive inhibitor 1NM-PP1. Paradoxically, rather than being inhibited by 1NM-PP1, drug-sensitized Ire1 mutants required 1NM-PP1 as a co-factor for activation. In the presence of 1NM-PP1, drug-sensitized Ire1 bypassed mutations that inactivate its kinase activity and induced a full UPR. Thus, rather than phosphorylation per se, a conformational change in the kinase domain triggered by occupancy of the active site with a ligand leads to activation of all known downstream functions.

Secretory and transmembrane proteins traversing the endoplasmic reticulum (ER) during their biogenesis fold to their native states in this compartment (*1*). This process is facilitated by a plethora of ER-resident activities (the protein folding machinery) (*2*). Insufficient protein folding capacity causes accumulation of unfolded proteins in the ER lumen (ER stress), and triggers a transcriptional program called the unfolded protein response (UPR). In yeast, UPR targets include genes encoding chaperones, oxido-reductases, phospholipid biosynthetic enzymes, ER-associated degradation (ERAD) components, and proteins functioning downstream in the secretory pathway (*3*). Together, UPR target activities afford proteins passing through the ER an extended opportunity to fold and assemble properly, dispose of unsalvageable unfolded polypeptides, and increase the capacity for ER export.

The yeast UPR is signaled through the ER stress sensor Ire1, a single-spanning ER transmembrane protein with three functional domains (*4*). The most amino-terminal domain, which resides in the ER lumen, senses elevated levels of unfolded ER proteins. Dissociation of ER chaperones from Ire1 as they become engaged with unfolded proteins is thought to trigger Ire1 activation (*3*).

Ire1's most carboxyl-terminal domain is a regulated endoribonuclease (RNase), which has a single known substrate in yeast: the $HAC1^u$ mRNA ('u' for uninduced), which encodes the Hac1 transcriptional activator necessary for activation of UPR targets (*5*). $HAC1^u$ mRNA is constitutively transcribed, but not translated, because it contains a non-conventional translation-inhibitory intron (*6*). Upon activation, Ire1's RNase cleaves $HAC1^u$ mRNA at two specific sites, excising the intron (*7*). The 5' and 3' exons are rejoined by tRNA ligase (*8*), resulting in spliced $HAC1^i$ mRNA ('i' for induced), which is actively translated to produce the Hac1 transcriptional activator, in turn upregulating UPR target genes (*5*).

A functional kinase domain precedes the RNase domain on the cytosolic side of the ER membrane (*9*). Activation of Ire1 leads to its oligomerization in the ER membrane, followed by *trans*-autophosphorylation (*9*, *10*). Mutations of catalytically essential kinase active site residues or residues known to become phosphorylated prevent $HAC1^u$ mRNA splicing and abrogate UPR signaling, demonstrating that Ire1's kinase phospho-transfer function is essential for RNase activation (*4*, *9*, *11*). Thus Ire1 communicates an unfolded protein signal from the ER to the cytosol using the lumenal domain as the sensor and the RNase domain as the effector. While clearly important for the circuitry of this machine, it is unknown why and how Ire1's kinase is required for activation of its RNase. To dissect the role of Ire1's kinase function, we have used a recently developed strategy that allows us to sensitize Ire1 to specific kinase inhibitors (*12*).

Unexpected behavior of Ire1 mutants sensitized to an ATP-competitive drug. Mutation of Leu745—situated at a conserved position in the ATP binding site—to Ala or Gly is predicted to sensitize Ire1 to the ATP-competitive drug 1-*tert*-butyl-3-naphthalen-1-ylmethyl-1*H*-pyrazolo[3,4-*d*]pyrimidin-4-ylamine (1NM-PP1) by creating an enlarged active site pocket not found in any wild-type kinase (*13*). Most kinases are not affected by these mutations, while others are partially or severely impaired (*14*, *15*). For Ire1, these substitutions markedly decreased UPR signaling—assayed through an in vivo reporter—indicative of decreased kinase activity. Ire1(L745A) showed a 40% decrease relative to wild-type,

whereas Ire1(L745G) showed a >90% decrease, approaching that of the Δ*ire1* control (Fig. 1A).

Unexpectedly, addition of 1NM-PP1 to cells expressing partially active Ire1(L745A) caused no inhibition, even at concentrations which completely inhibit other 1NM-PP1-sensitized kinases (*15*, *16*). Rather, 1NM-PP1 increased reporter activity slightly (Fig 1A, bar 4). To our further surprise, 1NM-PP1 provided to the severely crippled Ire1(L745G) significantly restored signaling (Fig. 1A, bar 6). This result presents a paradox: an ATP-competitive compound expected to function as an inhibitor of the rationally engineered mutant enzyme instead permits activation.

UPR activation strictly required induction by DTT (Fig. 1) or tunicamycin (*17*); 1NM-PP1 by itself had no effect, indicating that it does not induce the UPR by directly affecting ER protein folding. Moreover, the effects of 1NM-PP1 were specific: other structurally similar compounds, 2-naphthylmethyl PP1, a regio-isomer, and 1-naphthyl PP1, which lacks the methylene group between the heterocyclic ring and the naphthyl group, neither activated nor inhibited wild-type or mutant Ire1 (*17*).

Activation, rather than inhibition, by an ATP-competitive inhibitor raised the question of whether the kinase activity per se is necessary in the 1NM-PP1-sensitized mutants. To this end, we combined the L745A or L745G mutation with a 'kinase-dead' variant D828A, which lacks an active site Asp residue needed to chelate Mg^{2+} (*11*, *18*). While the Ire1(L745A,D828A) double mutant was detectable in cells at near wild-type levels (see below), Ire1(L745G,D828A) was undetectable—probably because of instability—and could not be assayed. As expected, Ire1(L745A,D828A) was unable to induce the UPR reporter with DTT alone, but addition of 1NM-PP1 allowed activation to levels approaching 80% of wild-type (Fig. 1B). This suggests that the binding of 1NM-PP1 to 1NM-PP1-sensitized Ire1 renders the kinase activity dispensable.

Trans-autophosphorylation by Ire1 of two activation segment Ser residues (S840 and S841) is necessary for signaling (*9*), prompting the question of whether this requirement is also bypassed in 1NM-PP1-sensitized mutants. As expected, the un-phosphorylatable Ire1(S840A,S841A) mutant was inactive in the absence and presence of 1NM-PP1 (Fig. 1C). In contrast, both the 1NM-PP1-sensitized Ire1(L745A,S840A,S841A) and Ire1(L745G,S840A,S841A) mutants were significantly activated by 1NM-PP1, indicating that phosphorylation of S840 and S841 can be bypassed. Two trends are apparent: with DTT alone, relative to the parent mutant Ire1(S840A,S841A), signaling decreased as the side chain of residue 745 was progressively reduced from leucine to alanine to glycine (Fig. 1C, bars 3,5,7). This is consistent with the results of Fig.1A that showed an increasing sensitivity of the active site to side chain reduction at residue 745. Reciprocally, in the presence of 1NM-PP1, activation of 1NM-PP1-sensitized Ire1(S840A,S841A) mutants increased in the same order (Fig. 1C, bars 4,6,8), perhaps due to progressively enhanced binding by 1NM-PP1 as the residue 745 side chain was trimmed back.

1NM-PP1-sensitized Ire1 requires 1NM-PP1 as a co-factor for *HAC1* mRNA splicing. We next confirmed that activation by 1NM-PP1-sensitized Ire1 mutants followed the expected pathway of activating *HAC1* mRNA splicing and Hac1 protein production. As expected, UPR induction of wild-type cells with DTT caused splicing of *HAC1* mRNA, as revealed by near-complete conversion of $HAC1^u$ to $HAC1^i$ mRNA (Fig. 2A, lanes 1 and 2) (*5*); 1NM-PP1 had no effect either by itself or with DTT (Fig. 2A, lanes 3 and 4). In strict correlation with *HAC1* mRNA splicing, Hac1 protein accumulated significantly (Fig. 2C, lanes 2 and 4).

By contrast, cells expressing 1NM-PP1-sensitized Ire1(L745G) spliced *HAC1* mRNA weakly with DTT alone, but displayed a significant increase when 1NM-PP1 was also provided (Fig. 2A, lanes 5–8). 1NM-PP1 alone did not activate *HAC1* mRNA splicing. As expected, Hac1 protein levels correlated with splicing (e.g., Fig. 2C, lanes 6 and 8). Activation by 1NM-PP1 was even more pronounced in cells expressing the Ire1(L745A,D828A) double mutant, which neither spliced *HAC1* mRNA nor produced Hac1 protein with DTT alone, but exhibited robust splicing and Hac1 protein production when provided both 1NM-PP1and DTT (Fig. 2A and C, compare lanes 10 and 12).

Importantly, steady-state levels of Ire1 proteins were comparable in all experiments, excluding as a trivial explanation for the observed effects the possibility that 1NM-PP1-sensitized Ire1 mutants are only stably expressed in the presence of 1NM-PP1 (Fig. 2D). Taken together our data show that 1NM-PP1 permits—but does not instruct—1NM-PP1-sensitized Ire1 mutants to splice *HAC1* mRNA in response to ER stress. Thus, in the genetic background of 1NM-PP1-sensitized *IRE1* alleles, 1NM-PP1 is, in effect, a co-factor for signaling in the UPR.

1NM-PP1 uncouples the kinase and RNase activities of 1NM-PP1-sensitized Ire1. To rule out indirect effects, we assayed the activities of the Ire1 mutants described above in vitro. The cytosolic portion of Ire1 consisting of the kinase domain and RNase domain (Ire1*) was expressed and purified from *E. coli* (*7*). Using [γ-^{32}P] labeled ATP, we assayed wild-type Ire1* and Ire1*(L745G) for autophosphorylation in the presence or absence of 1NM-PP1. Wild-type Ire1* exhibited strong autophosphorylation, which was not inhibited by 1NM-PP1 (Fig. 3A, lanes 1 and 2). In contrast, Ire1*(L745G) exhibited markedly diminished autophosphorylation—consistent with poor signaling by Ire1(L745G) in vivo (Figs. 1 and 2)—which was completely

extinguished by 1NM-PP1 (Fig. 3A, lane 3 and 4). This suggested that Ire1*(L745G) is diminished in its ability to use ATP as substrate and that 1NM-PP1 is, as predicted, an ATP competitor.

By contrast, when provided [γ-^{32}P]-labeled *N-6* benzyl ATP—an ATP analog with a bulky substituent (Fig. 3E)—Ire1*(L745G) displayed enhanced autophosphorylation activity relative to wild-type Ire1* (Fig. 3B, lane 1 and 2). Therefore the L745G mutation does not destroy Ire1's catalytic function, but rather alters its substrate specificity from ATP to ATP analogs having complementary features that permit binding in the expanded active site.

To ask how the RNase activity of Ire1 is affected by manipulation of its kinase domain, we incubated wild-type and Ire1*(L745G) with a truncated in vitro transcribed *HAC1* RNA substrate ($HAC1_{600}$) and monitored production of cleavage products (*7*). Wild-type Ire1* cleaved $HAC1_{600}$ RNA at both splice junctions, producing the expected fragments corresponding to the singly and doubly cut species (Fig. 3C, lane 2). The cleavage reaction was not affected by 1NM-PP1 (Fig. 3C, lane 3). In contrast, Ire1*(L745G) was completely inactive, while addition of 1NM-PP1—at the same concentration that was shown in Figure 3A (lane 4) to completely inhibit the kinase activity—restored RNase activity significantly (Fig. 3C, lanes 4 and 5), strongly supporting the notion that 1NM-PP1 uncouples the kinase and RNase activities of 1NM-PP1-sensitized Ire1.

We previously showed that cleavage of *HAC1* mRNA by wild-type Ire1* is stimulated by ADP (*7*). This is consistent with the notion derived from in vivo studies that Ire1 requires an active kinase domain, because we know that recombinant wild-type Ire1* is already phosphorylated, thereby alleviating a necessity for de novo phosphorylation in vitro. ADP efficiently stimulated the RNase activity of Ire1* (Fig. 3D, lane 1) but not that of Ire1*(L745G) (Fig. 3D, lane 2).

For wild-type Ire1 and 1NM-PP1-sensitized Ire1(L745G) therefore, ADP and 1NM-PP1 respectively function as stimulatory co-factors. Therefore we asked whether a conformational change occurs in response to co-factor binding by analyzing Ire1* and Ire1*(L745G) through glycerol gradient velocity sedimentation. Ire1* sedimented as a broad peak in the gradient (Fig. 4). Upon addition of ADP (Fig. 4B), but not 1NM-PP1 (Fig. 4C), the peak shifted to a higher S value. Conversely, the peak of Ire1*(L745G) shifted by a corresponding amount upon addition of 1NM-PP1 (Fig. 4F) but not upon addition of ADP (Fig. 4E). This shift may be indicative of a conformational change and/or change in the oligomeric state of the enzymes in response to binding of their respective co-factors.

1NM-PP1-sensitized, kinase-dead Ire1 signals a canonical UPR. To ask whether bypassing the Ire1 kinase activity with 1NM-PP1 allows induction of a full UPR, we profiled mRNA expression on yeast genomic microarrays. To this end, mRNA from wild-type *IRE1*, Δ*ire1*, and *IRE1*(L745A,D828A) cells were isolated at different time points after addition of 1NM-PP1 and DTT. cDNA's derived from these mRNA populations were labeled with different fluorescent dyes, mixed pair-wise and hybridized to microarrays (*19*). Scatter plots of pair-wise comparisons of mRNA expression levels are shown in Figure 5; the x-y scatter plots represent relative expressions for every mRNA between the specified genotypes.

Comparison of wild-type *IRE1*-expressing cells with Δ*ire1* cells revealed a distinct set of upregulated UPR target genes in wild-type *IRE1*-expressing cells (Fig. 5A; genes upregulated more than 2-fold in pink). These *IRE1*-dependent genes include previously described UPR transcriptional targets (*20*, *21*). Strikingly, the same set of (pink-colored) UPR target genes was upregulated to a similar magnitude in *IRE1*(L745A,D828A)-expressing cells relative to Δ*ire1* cells (Fig. 5B), suggesting that a canonical UPR was induced in the 1NM-PP1-sensitized, kinase-dead mutant. This conclusion was confirmed by the tight superimposition of the scatter diagonals of both UPR targets and the rest of the transcriptome evident in the expression profiles of wild-type *IRE1* vs. *IRE1*(L745A,D828A)-expressing cells (Fig. 5C).

Building an instructive UPR switch. The 1NM-PP1-sensitized *IRE1* mutants described so far act permissively, since activation requires both 1NM-PP1 and protein misfolding agents. This indicates that an unfolded protein signal needs to be received by the ER-lumenal domain for activation. We asked if we could bypass this requirement using a constitutively-on version of *IRE1* (called $IRE1^C$) isolated previously through random mutagenesis of the ER-lumenal domain (*17*, *20*). $IRE1^C$ significantly induced the UPR without DTT —approximately 75% of the maximal activity of wild-type *IRE1* with DTT (Fig. 1D, bars 2 and 5). We predicted that a chimera of the $IRE1^C$ and 1NM-PP1-sensitized, kinase-dead *IRE1*(L745A,D828A) mutants would activate the UPR with 1NM-PP1 alone—even in the absence of DTT. The data in Figure 1D (bars 13–16) show that this prediction holds true. Whereas wild-type *IRE1* requires DTT for induction and is immune to 1NM-PP1 (Fig. 1D, bars 1–4), and *IRE1*(L745A,D828A) requires both DTT and 1NM-PP1 (Fig. 1D, bars 9–12), the chimeric $IRE1^C$ (L745A,D828A) requires only 1NM-PP1 for activation irrespective of addition of DTT (Fig. 1D, bars 13–16). Thus, $IRE1^C$ (L745A,D828A) is an instructive switch that turns on the UPR upon addition of 1NM-PP1 alone (i.e. even in the absence of ER stress).

Summary and implications. Since our discovery that Ire1's RNase initiates splicing of *HAC1* mRNA, the function of its kinase domain has remained an enigma (*7*). While mutational analyses indicated a requirement for an enzymatically active kinase and defined activation segment

phosphorylation sites (*9*), to date no targets besides Ire1 itself have been identified. Here we report that both the kinase activity and activation segment phosphorylation can be bypassed if the small ATP-mimic 1NM-PP1 is provided to a mutant enzyme to which it can bind. Rather than inhibiting the function served by ATP, 1NM-PP1 rectifies the signaling defect of 1NM-PP1-sensitized Ire1 mutants, leading to induction of a canonical UPR (*20*). Thus, ligand binding to the kinase domain, rather than a phosphotransfer function mediated by the kinase activity per se, is required for RNase activation. The kinase module of Ire1, therefore, uses an unprecedented mechanism to propagate the UPR signal.

One model that could explain our data is proposed in Figure 6B. According to this model, autophosphorylation of wild-type Ire1 occurs in *trans* between Ire1 molecules after they have been released from their chaperone anchors and have oligomerized by lateral diffusion in the plane of the ER membrane (*9*, *22*). *Trans*-autophosphorylation of the activation segment locks the activation segment in the "swung-out" state (*23*, *24*), and fully opens the active site, allowing ADP or ATP to bind efficiently, leading in turn to conformational changes that activate the RNase domain.

By contrast, binding of 1NM-PP1 to the active site of 1NM-PP1-sensitized Ire1 occurs even in the absence of phosphorylation of the activation segment. It is plausible that because of its small size, 1NM-PP1 can bypass the "closed" activation segment—proposed to occlude access to the active site for the larger ADP and ATP molecules (Fig. 6A). Alternatively, 1NM-PP1 may enter the active site when the unphosphorylated activation segment opens transiently, which occurs with low frequency in other kinases (*25*). If the off-rate of 1NM-PP1 binding to 1NM-PP1-sensitized Ire1 is slow compared to that of ADP and ATP, most mutant Ire1 molecules could be trapped in a drug-bound state. Based on either scenario, we propose that drug binding alone causes conformational rearrangements in the kinase that activate the RNase. The nucleotide-bound state of phosphorylated wild-type Ire1, therefore, mimics the 1NM-PP1-bound state of unphosphorylated 1NM-PP1-sensitized Ire1. The model discussed so far does not explain why 1NM-PP1 should not bind to individual 1NM-PP1-sensitized Ire1 molecules and activate them, even without oligomerization induced by activation of the UPR through the ER lumenal domain. Two possibilities could account for the observations: i) binding of 1NM-PP1 may be enhanced in oligomerized, chaperone-free mutant, or ii) 1NM-PP1 may bind equally well to chaperone-anchored and chaperone-free (or constitutive-on) Ire1, but oligomerization may be required because interaction between neighboring molecules is required for the conformational change that activates the RNase function. Currently, our data do not allow us to distinguish between these possibilities.

Our findings provoke the question of what the "natural" stimulatory ligand of Ire1's kinase domain may be. One likely candidate is ADP, which is generated by Ire1 from ATP during the autophosphorylation reaction. In vitro, ADP is a better activator of Ire1 than ATP (*7*). Ire1 would therefore be "self-priming", generating an efficient activator already bound to its active site. In many professional secretory cells such as the β-cells of the endocrine pancreas (which contain high concentrations of Ire1), ADP levels rise (and ATP levels decline) temporarily in proportion to nutritional stress (*26*). ADP therefore is physiologically poised to serve as a co-factor that could signal a starvation state. It is known that protein folding becomes inefficient as the nutritional status of cells declines, triggering the UPR (*27*). Thus in the face of ATP depletion, ADP-mediated conformational changes might increase the dwell time of activated Ire1. As such, Ire1 could have evolved this regulatory mechanism to monitor the energy balance of the cell, and couple this information to activation of the UPR.

While unprecedented in proteins containing active kinase domains, our findings are consistent with previous observations on RNase L, which is closely related to Ire1, bearing a kinase-like domain followed C-terminally by an RNase domain (*28*, *29*). Like Ire1, RNase L is activated by dimerization (*30*). However, RNase L's kinase domain is naturally inactive (*28*), while its RNase activity is stimulated by adenosine nucleotide binding to the kinase domain. Therefore, like Ire1, the ligand-occupied kinase domain of RNase L serves as a module that participates in activation and regulation of the RNase function. Insights gained from Ire1 and RNase L may extend to other proteins containing kinase or enzymatically inactive pseudokinase domains (*31*).

References and Notes

1. M. J. Gething, J. Sambrook, *Nature* **355**, 33 (1992).
2. F. J. Stevens, Y. Argon, *Semin. Cell Dev. Biol.* **10**, 443 (1999).
3. C. Patil, P. Walter, *Curr. Opin. Cell Biol.* **13**, 349 (2001).
4. J. S. Cox, C. E. Shamu, P. Walter, *Cell* **73**, 1197 (1993).
5. J. S. Cox, P. Walter, *Cell* **87**, 391 (1996).
6. U. Ruegsegger, J. H. Leber, P. Walter, *Cell* **107**, 103 (2001).
7. C. Sidrauski, P. Walter, *Cell* **90**, 1031 (1997).
8. C. Sidrauski, J. S. Cox, P. Walter, *Cell* **87**, 405 (1996).
9. C. E. Shamu, P. Walter, *EMBO J.* **15**, 3028 (1996).
10. A. Weiss, J. Schlessinger, *Cell* **94**, 277 (1998).
11. K. Mori, W. Ma, M. J. Gething, J. Sambrook, *Cell* **74**, 743 (1993).
12. K. Shah, Y. Liu, C. Deirmengian, K. M. Shokat, *Proc. Natl. Acad. Sci. U.S.A.* **94**, 3565 (1997).
13. A. C. Bishop *et al.*, *Curr. Biol.* **8**, 257 (1998).
14. E. L. Weiss, A. C. Bishop, K. M. Shokat, D. G. Drubin, *Nature Cell Biol.* **2**, 677 (2000).

15. A. C. Bishop *et al.*, *Nature* **407**, 395 (2000).
16. A. S. Carroll, A. C. Bishop, J. L. DeRisi, K. M. Shokat, E. K. O'Shea, *Proc. Natl. Acad. Sci. U.S.A.* **98**, 12578 (2001).
17. Data not shown.
18. M. Huse, J. Kuriyan, *Cell* **109**, 275 (2002).
19. J. L. DeRisi, V. R. Iyer, P. O. Brown, *Science* **278**, 680 (1997).
20. K. J. Travers *et al.*, *Cell* **101**, 249 (2000).
21. Supporting online material
22. F. Urano, A. Bertolotti, D. Ron, *J. Cell Sci.* **113**, 3697 (2000).
23. S. R. Hubbard, M. Mohammadi, J. Schlessinger, *J. Biol. Chem.* **273**, 11987 (1998).
24. T. Schindler *et al.*, *Mol. Cell* **3**, 639 (1999).
25. M. Porter, T. Schindler, J. Kuriyan, W. T. Miller, *J. Biol. Chem.* **275**, 2721 (2000).
26. F. Schuit, K. Moens, H. Heimberg, D. Pipeleers, *J. Biol. Chem.* **274**, 32803 (1999).
27. R. J. Kaufman *et al.*, *Nature Rev. Mol. Cell Biol.* **3**, 411 (2002).
28. B. Dong, M. Niwa, P. Walter, R. H. Silverman, *RNA* **7**, 361 (2001).
29. S. Naik, J. M. Paranjape, R. H. Silverman, *Nucleic Acids Res.* **26**, 1522 (1998).
30. B. Dong, R. H. Silverman, *Nucleic Acids Res.* **27**, 439 (1999).
31. M. Kroiher, M. A. Miller, R. E. Steele, *Bioessays* **23**, 69 (2001).
32. We thank Martha Stark for constructing the *IRE1*^{C} allele and Scott Ullrich for his initial effort in constructing Ire1 mutants. We also thank John Kuriyan and members of the Walter and Shokat labs for many valuable discussions. This work was supported by grants from the NIH to PW (GM32384) and KS (AI44009), and postdoctoral support from the UCSF Molecular Medicine Program to FP. PW receives support as an investigator of the Howard Hughes Medical Institute.

Supporting Online Material

www.sciencemag.org/cgi/content/full/1090031/DC1
Materials and Methods
Microarray Excel Spreadsheets S1 to S3
References and Notes

4 August 2003; accepted 1 October 2003
Published online 16 October 2003; 10.1126/science.1090031
Include this information when citing this paper.

Fig. 1. In vivo UPR assays using a UPRE-driven *lacZ* reporter. The relevant genotypes and the presence or absence of 1NM-PP1 and the UPR inducer DTT are indicated. For (**A**-**C**), DTT was used in all assays.

Fig. 2. In vivo *HAC1* mRNA splicing and Hac1 protein production. Northern blots (**A**) showing in vivo *HAC1* mRNA splicing, and (**B**) *SCR1* rRNA as loading control. Western blots showing Hac1 (**C**) and Ire1 protein levels (**D**). The arrow in (C), lane 6, calls attention to the small amount of Hac1 protein present in these cells.

Fig. 3. In vitro assays of Ire1 mutant proteins. Ire1* autophosphorylation assays using [γ-^{32}P] ATP (**A**) and [γ-^{32}P]-labeled *N-6* benzyl ATP (**B**)**.** Phosphorylated-Ire1* proteins (wild-type and L745G) are indicated. Ire1* RNase assays (against in vitro transcribed $HAC1_{600}$ RNA) using stimulatory co-factors 1NM-PP1 in (**C**) and ADP in (**D**). Icons in (C) and (D) indicate $HAC1_{600}$ RNA cleavage products, denoting all combinations of singly and doubly cut RNA. (**E**) The chemical structures of 1NM-PP1 and *N-6* benzyl ATP are shown.

Fig. 4. Glycerol density gradient velocity sedimentation of wildtype and mutant Ire1*. Ire1* and Ire1(L745G)* proteins were incubated in the presence of ADP or 1NM-PP1 as indicated and subjected to velocity sedimentation analysis. Sedimentation is from left to right.

Fig. 5. x-y scatter plot analysis of mRNA abundance. The plots (log_{10}) compare yeast genomic microarray analyses between the genotypes indicated. In each case, mRNA was purified from cells provided both DTT and 1NM-PP1. Pink dots represent genes more than 2-fold higher expression in wild-type cells relative to Δ*ire1* cells.

Fig. 6. Model of activation of 1NM-PP1-sensitized and wild-type Ire1. For both proteins, chaperone dissociation due to unfolded protein accumulation causes oligomerization in the plane of the ER membrane, which is a precondition for further activation. For mutant Ire1 (**A**), 1NM-PP1 binding to the inactive kinase domain active site causes a conformational change, which activates the RNase. For wild-type Ire1 (**B**), *trans*-autophosphorylation, using ATP, of the activation segment fully opens the kinase domain for binding of ADP or ATP, which activates the RNase.

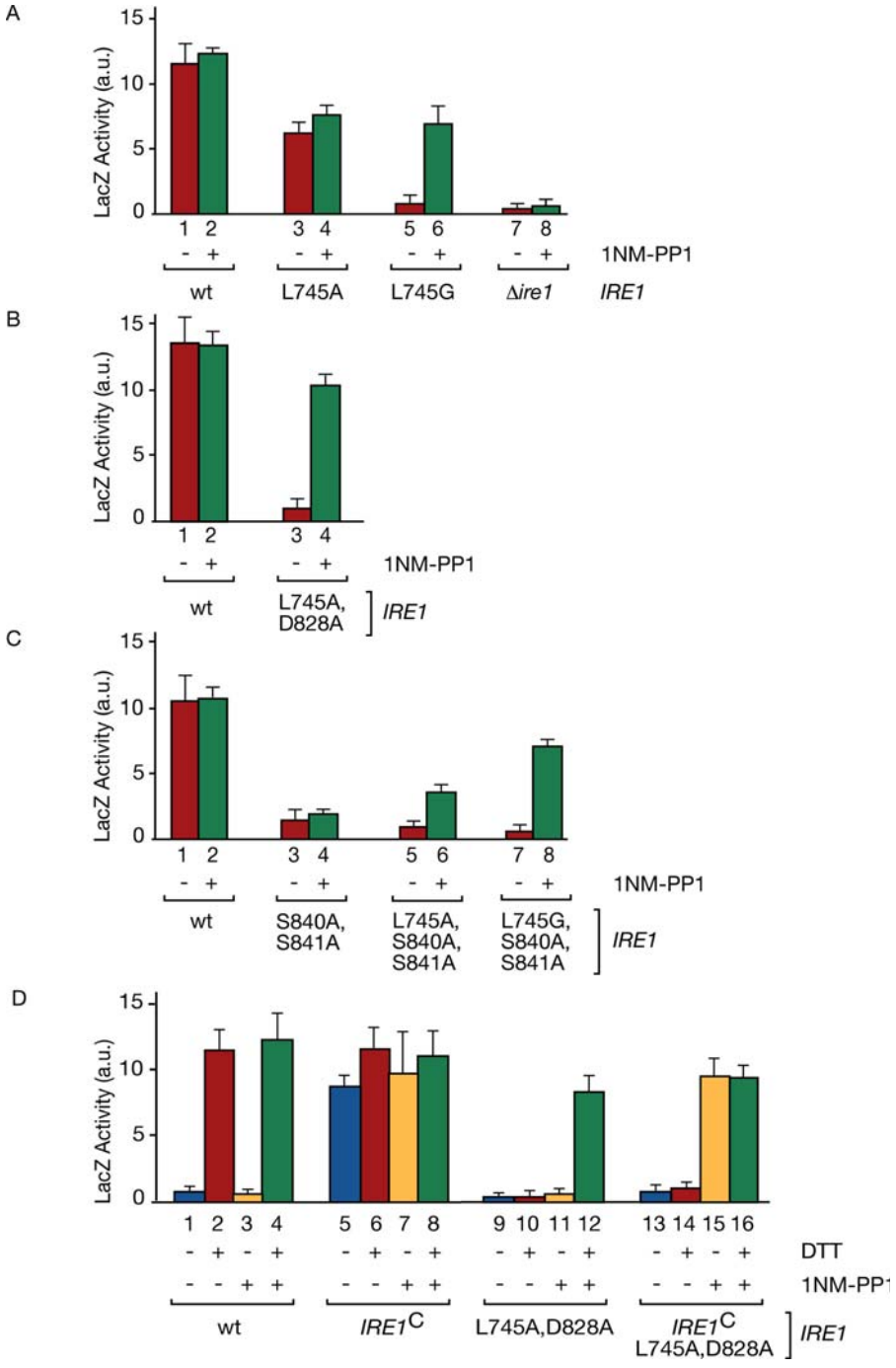
A
LacZ Activity (a.u.)
15
10
5
0
1 2 3 4 5 6 7 8
- + - + - + - +
1NM-PP1
wt
L745A
L745G
Δire1
IRE1
B
LacZ Activity (a.u.)
1 2 3 4
- + - +
1NM-PP1
wt
L745A, D828A
IRE1
C
LacZ Activity (a.u.)
1 2 3 4 5 6 7 8
- + - + - + - +
1NM-PP1
wt
S840A, S841A
L745A, S840A, S841A
L745G, S840A, S841A
IRE1
D
LacZ Activity (a.u.)
1 2 3 4 5 6 7 8 9 10 11 12 13 14 15 16
DTT
1NM-PP1
wt
IRE1C
L745A,D828A
IRE1C L745A,D828A
IRE1

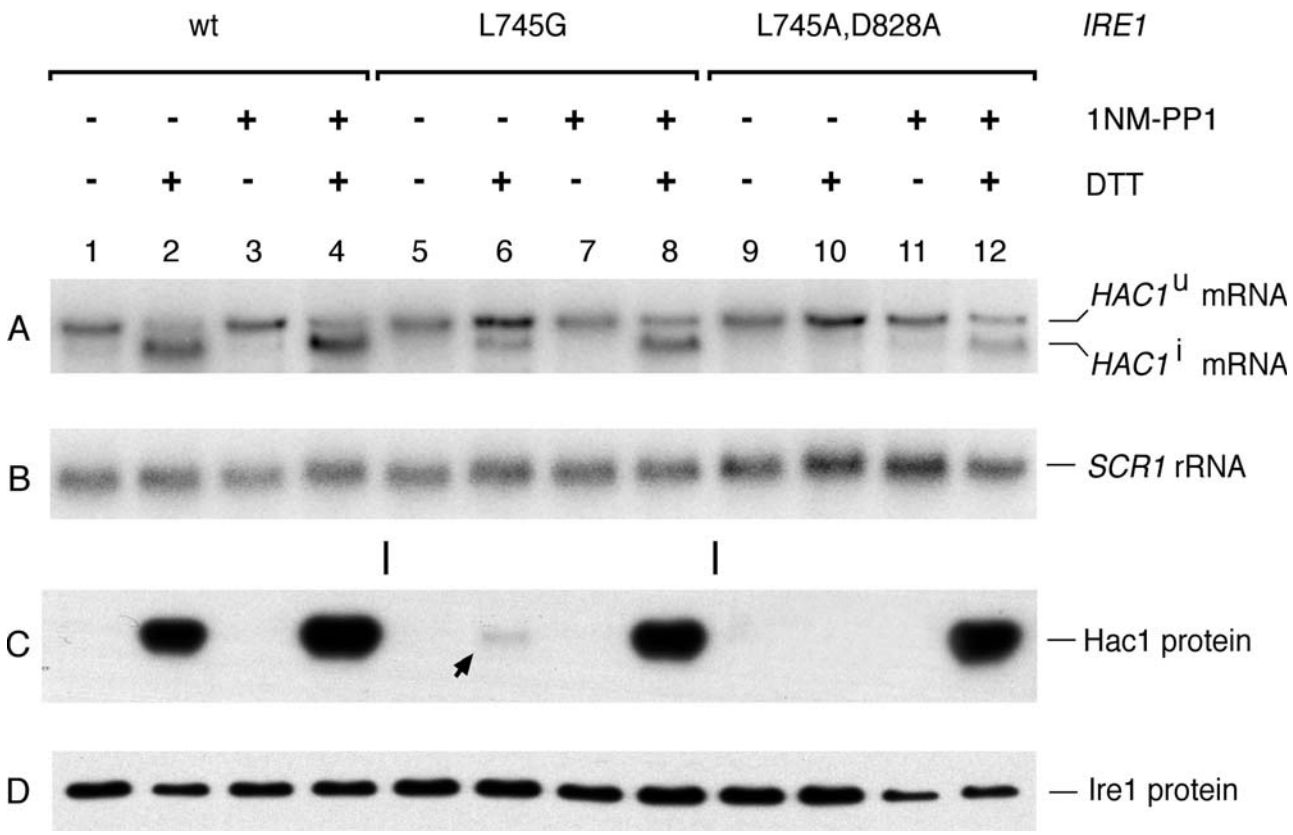
wt
L745G
L745A,D828A
IRE1
- - + + - - + + - - + + 1NM-PP1
- + - + - + - + - + - + DTT
1 2 3 4 5 6 7 8 9 10 11 12
A
HAC1u mRNA
HAC1i mRNA
B
SCR1 rRNA
C
Hac1 protein
D
Ire1 protein

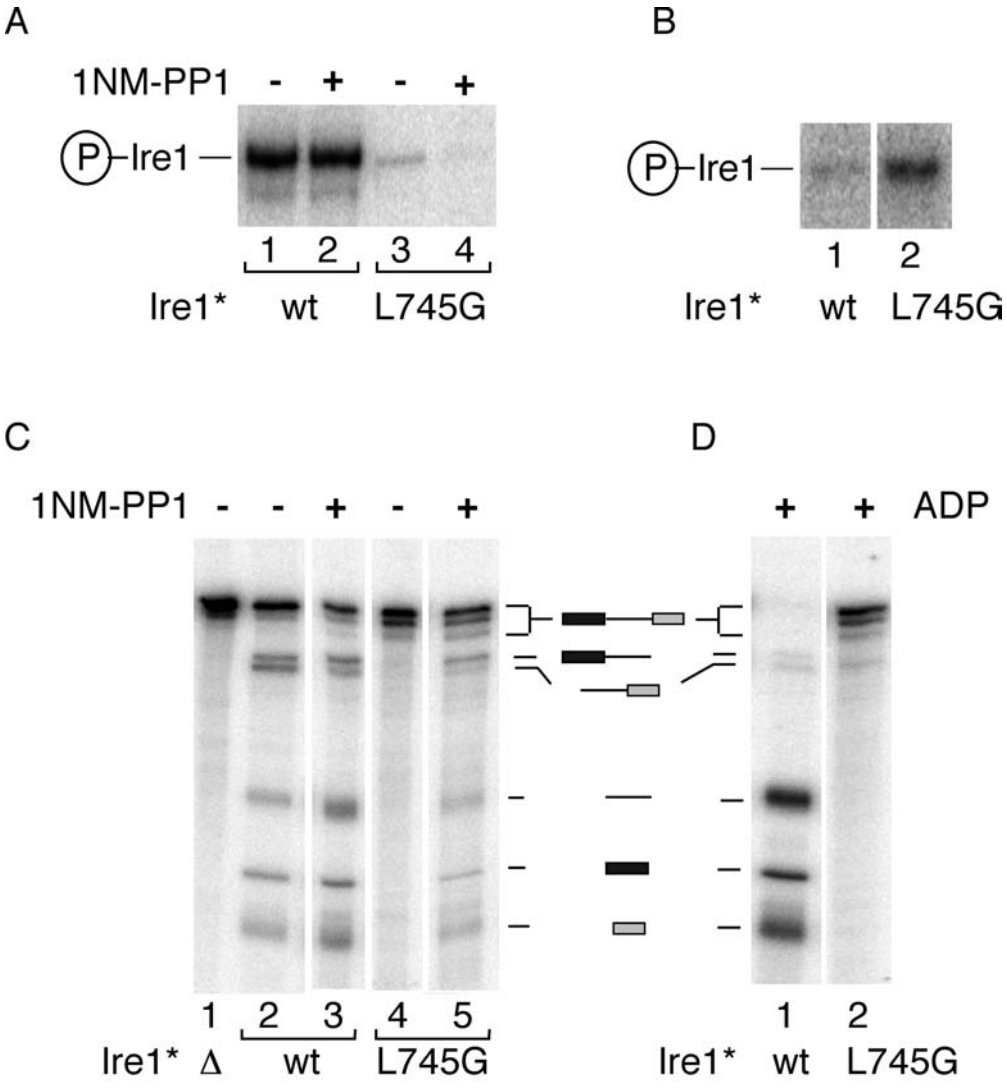
A
1NM-PP1 - + - +
P-Ire1
1 2 3 4
Ire1* wt L745G
B
P-Ire1
1 2
Ire1* wt L745G
C
1NM-PP1 - - + - +
1 2 3 4 5
Ire1* Δ wt L745G
D
+ + ADP
1 2
Ire1* wt L745G
E
1NM-PP1
NH2
N
N
N
N
N-6 benzyl ATP
HN
N
N
N
N
HO-P-O-P-O-P-O
O
OH OH OH
O
OH OH

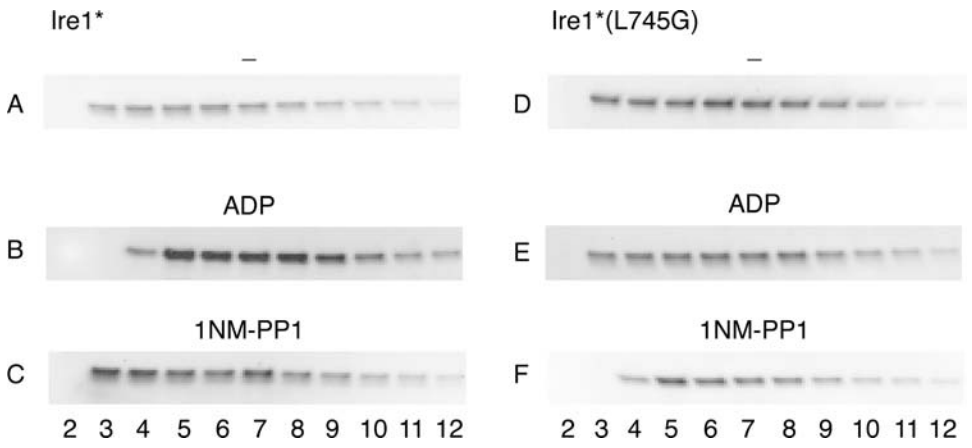
Ire1*
Ire1*(L745G)
–
A
D
ADP
B
E
1NM-PP1
C
F
2 3 4 5 6 7 8 9 10 11 12
2 3 4 5 6 7 8 9 10 11 12

A

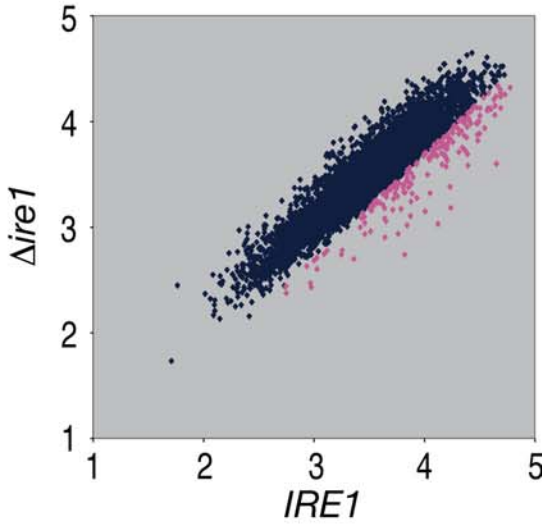
5
4
3
2
1
Δire1
1
2
3
4
5
IRE1

B

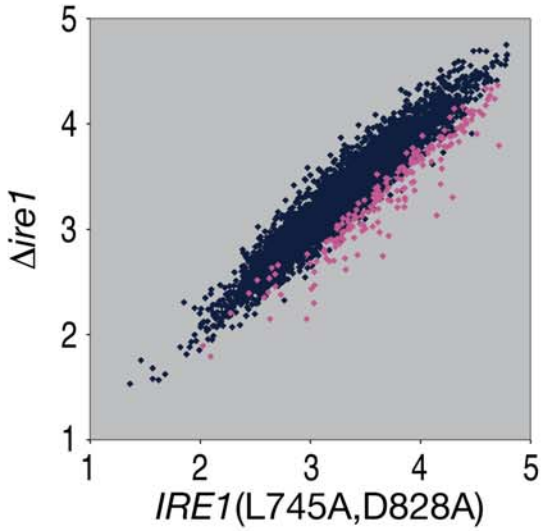
5
4
3
2
1
Δire1
1
2
3
4
5
IRE1(L745A,D828A)

C

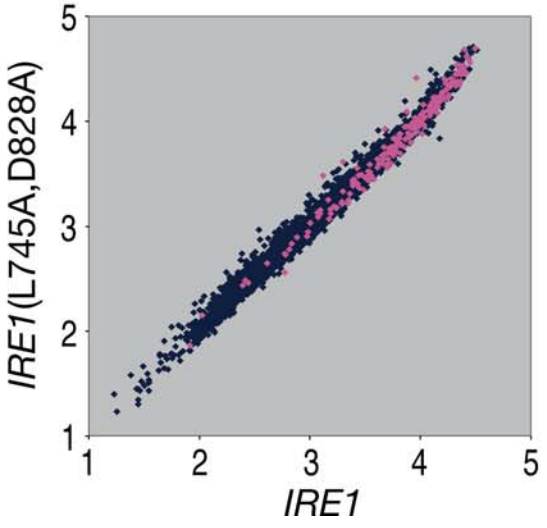
5
4
3
2
1
IRE1(L745A,D828A)
1
2
3
4
5
IRE1

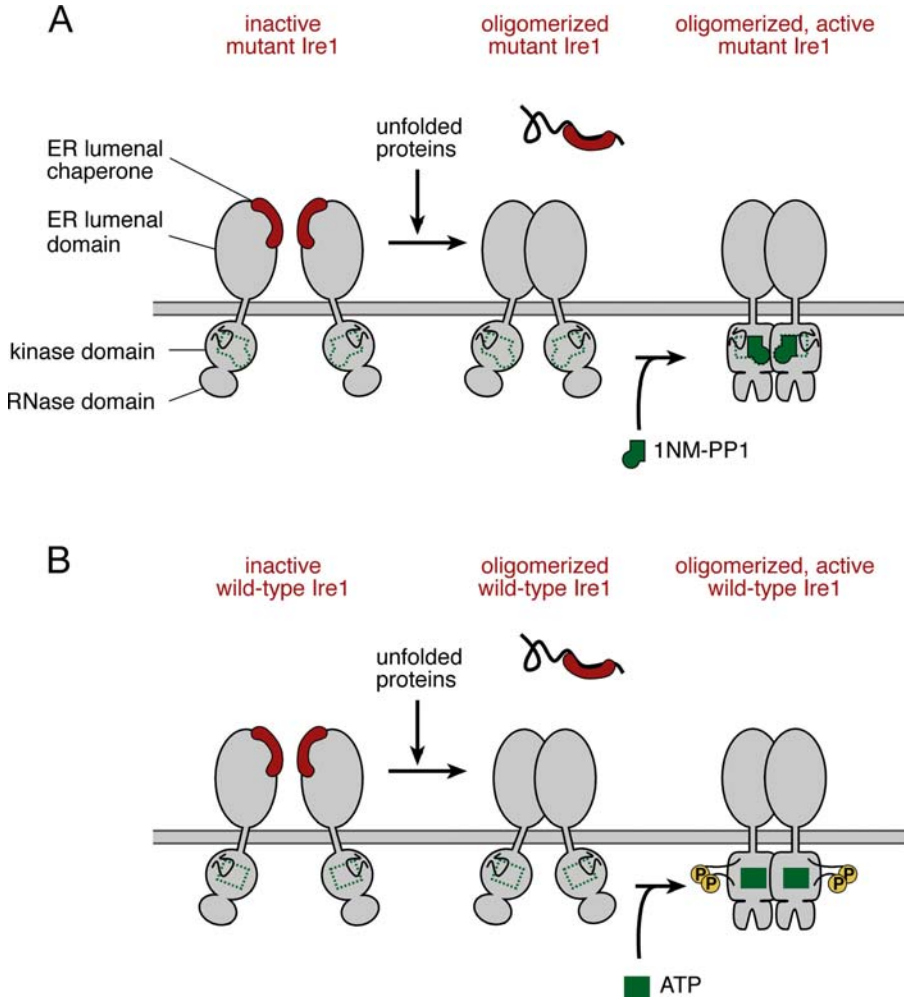
A
inactive
mutant Ire1
oligomerized
mutant Ire1
oligomerized, active
mutant Ire1
unfolded
proteins
ER lumenal
chaperone
ER lumenal
domain
kinase domain
RNase domain
1NM-PP1
B
inactive
wild-type Ire1
oligomerized
wild-type Ire1
oligomerized, active
wild-type Ire1
unfolded
proteins
P
P
P
P
ATP